Higgs couplings at the LHC

Dieter Zeppenfeld*
Department of Physics, University of Wisconsin, Madison, WI 53706, USA
(Dated: May 29, 2002)

The observation of a SM-like Higgs boson in multiple channels at the LHC allows the extraction of Higgs couplings to gauge bosons and fermions. The precision achievable at the LHC, for an integrated luminosity of 200 fb^{-1}, is reviewed and updated.

I. COUPLING DETERMINATION AT THE LHC

One of the prime tasks of the LHC will be to probe the mechanism of electroweak gauge symmetry breaking. Beyond observation of the various CP even and CP odd scalars which nature may have in store for us [1–3], this means the determination of the couplings of the Higgs boson to the known fermions and gauge bosons, i.e. the measurement of Htt, Hbb, $H\tau\tau$ and HWW, HZZ, $H\gamma\gamma$, Hgg couplings, to the extent possible.

Clearly this task very much depends on the expected Higgs boson mass. For $m_H > 200$ GeV and within the SM, only the $H \to ZZ$ and $H \to WW$ channels are expected to be observable, and the two gauge boson modes are related by SU(2). A much richer spectrum of decay modes is predicted for the intermediate mass range, i.e. if a SM-like Higgs boson has a mass between the LEP2 limit of 114 GeV and the Z-pair threshold. The main reasons for focusing on this range are present indications from electroweak precision data, which favor $m_H \lesssim 200$ GeV [4], as well as expectations within the MSSM, which predicts the lightest Higgs boson to have a mass $m_h \lesssim 135$ GeV. In this contribution I update and extend recent predictions for Higgs coupling measurements at the LHC [5] for a Higgs boson with couplings qualitatively similar to the SM case.

II. SURVEY OF INTERMEDIATE MASS HIGGS CHANNELS

The total production cross section for a SM Higgs boson at the LHC is dominated by the gluon fusion process, $gg \to H$, which largely proceeds via a top-quark loop. Thus, inclusive Higgs searches will collectively be called "gluon fusion" channels in the following. Three inclusive channels are highly promising for the SM Higgs boson search [1–3],

$$gg \to H \to \gamma\gamma\ , \qquad \text{for} \quad m_H \lesssim 150 \text{ GeV}\ , \tag{1}$$

$$gg \to H \to ZZ^* \to 4\ell\ , \qquad \text{for} \quad m_H \gtrsim 120 \text{ GeV}\ , \tag{2}$$

and

$$gg \to H \to WW^* \to \ell\bar{\nu}\bar{\ell}\nu\ , \qquad \text{for} \quad m_H \gtrsim 130 \text{ GeV}\ . \tag{3}$$

The $H \to \gamma\gamma$ signal can be observed as a narrow and high statistics $\gamma\gamma$ invariant mass peak, albeit on a very large diphoton background. A few tens of $H \to ZZ^* \to 4\ell$ events are expected to be visible in 100 fb^{-1} of data, with excellent signal to background ratios (S/B), ranging between 1:1 and 6:1, in a narrow four-lepton invariant mass peak. Finally, the $H \to WW^* \to \ell\bar{\nu}\bar{\ell}\nu$ mode is visible as a broad enhancement of event rate in a 4-lepton transverse mass distribution, with S/B between 1:4 and 1:1 (for favorable values of the Higgs mass, around 170 GeV). Analyses of these inclusive channels have been performed by CMS and ATLAS at the hadron level and include full detector simulations. These complete analyses were used as input in Ref. [5]. Expected accuracies for the three inclusive channels are shown as solid lines in Fig. 1.

Additional and crucial information on the Higgs boson can be obtained by isolating Higgs production in weak boson fusion (WBF), i.e. by separately observing $qq \to qqH$ and crossing related processes, in which the Higgs is radiated off a t-channel W or Z. Specifically, it was shown in parton level analyses that the weak boson fusion channels, with subsequent Higgs decay into photon pairs [6, 7],

$$qq \to qqH,\ H \to \gamma\gamma\ , \qquad \text{for} \quad m_H \lesssim 150 \text{ GeV}\ , \tag{4}$$

*dieter@pheno.physics.wisc.edu

TABLE I: Number of events expected for $qq \to qqH,\ H \to WW^* \to ll'\not{p}_T$ in 200 fb^{-1} of data, and corresponding backgrounds. Predictions for $m_H \geq 150$ GeV include $H \to WW^* \to \mu^\pm e^\mp \not{p}_T$ decays only [10]. For smaller Higgs boson masses, $H \to WW^* \to \mu^+\mu^- \not{p}_T,\ e^+e^- \not{p}_T$ decays are considered in addition (see Ref.[11]). The expected relative statistical error on the signal cross section, determined as $\sqrt{N_S+N_B}/N_S$, is given in the last line.

m_H	110	115	120	130	140	150	160	170	180	190
N_S	102	188	324	740	1226	908	1460	1436	1172	832
N_B	164	188	208	254	300	216	240	288	300	324
$\Delta\sigma_H/\sigma_H$	16.0%	10.3%	7.1%	4.3%	3.2%	3.7%	2.8%	2.9%	3.3%	4.1%

into $\tau^+\tau^-$ pairs [7–9],

$$qq \to qqH,\ H \to \tau\tau\ , \qquad \text{for} \quad m_H \lesssim 150 \text{ GeV}\ , \tag{5}$$

or into W pairs [7, 10, 11]

$$qq \to qqH,\ H \to WW^* \to e^\pm\mu^\mp \not{p}_T\ , \qquad \text{for} \quad m_H \gtrsim 110 \text{ GeV}\ , \tag{6}$$

can be isolated at the LHC. The weak boson fusion channels utilize the significant background reductions which are expected from double forward jet tagging and central jet vetoing techniques, and promise low background environments in which Higgs decays can be studied in detail.

Compared to the analysis of Ref. [5], new results for $H \to WW^* \to l^+\nu l'^-\bar{\nu}$ have become available [11] and will be included in the following. Table I summarizes expected event rates (after cuts and including efficiency factors) for the combined $qq \to qqH,\ H \to WW^* \to ll'\not{p}_T$ channels. The rates and ensuing statistical errors of the signal cross section are given for 100 fb^{-1} of data collected in both the ATLAS and the CMS detector.

The results used in this analysis for the WBF channels were derived at the parton level. First hadron level analyses with full detector simulation qualitatively confirm the parton level results [12], but yield somewhat lower rates. This can partially be explained by initial and final state radiation which produces additional jet activity, leading to misidentified forward tagging jets. A full simulation of forward jets confirms previous assumptions on jet reconstruction efficiencies which were based on a fast detector simulation. Lower efficiencies are found in the very far forward region only, which contributes little to the signal. The parton level results include jet reconstruction efficiencies of 0.86 per jet. Another effect of additional hadronic activity in the full simulation is a somewhat reduced reconstruction efficiency for isolated leptons, which was assumed to be 0.95 per lepton in the parton level studies. Finally, central jet veto efficiencies, as calculated in PYTHIA versus the parton level, approximately agree for the signal but show discrepancies for multi-jet QCD backgrounds, perhaps because PYTHIA uses $2 \to 2$ processes for the simulation of hard matrix elements. In view of these unresolved issues, the agreement between parton level and full simulation results, at the factor 2 level or better, is reassuring. Also, the parton level analysis did not make use of all decay channels (e.g. no $\tau^+\tau^- \to e^+e^-,\ \mu^+\mu^- + \not{p}_T$ decays), the full detector simulation for $H \to WW^*$ has not yet been optimized for $m_H \lesssim 140$ GeV, and no analysis has yet exploited multivariate techniques to enhance the Higgs signals over backgrounds. In light of this, the parton level results on WBF processes appear to be quite realistic and I use them in the following. Expected accuracies for the three WBF channels are shown as dashed lines in Fig. 1.

Among the associated production channels, $t\bar{t}H$ production appears most promising. Recent analyses have significantly improved the techniques for observing the decays into $b\bar{b}$ pairs [13, 14],

$$gg, q\bar{q} \to t\bar{t}H,\ H \to b\bar{b};\ , \qquad \text{for} \quad m_H \lesssim 130 \text{ GeV}\ , \tag{7}$$

and W^+W^- pairs [15],

$$gg, q\bar{q} \to t\bar{t}H,\ H \to W^+W^-\ , \qquad \text{for} \quad m_H \gtrsim 140 \text{ GeV}\ . \tag{8}$$

The $H \to b\bar{b}$ signal in $t\bar{t}H$ events will be visible with good purity, S/B $\approx 2/3$ [13], and the Higgs invariant mass peak allows for a direct measurement of backgrounds in the sidebands. The $H \to W^+W^-$ signal is expected to yield similar purity, but is more difficult to measure precisely, because the Higgs mass peak cannot be reconstructed. This makes precise background determinations challenging. A third associated production channel which has been re-analyzed recently is WH production [16],

$$q\bar{q} \to WH,\ H \to b\bar{b}\ , \qquad \text{for} \quad m_H \lesssim 120 \text{ GeV}\ . \tag{9}$$

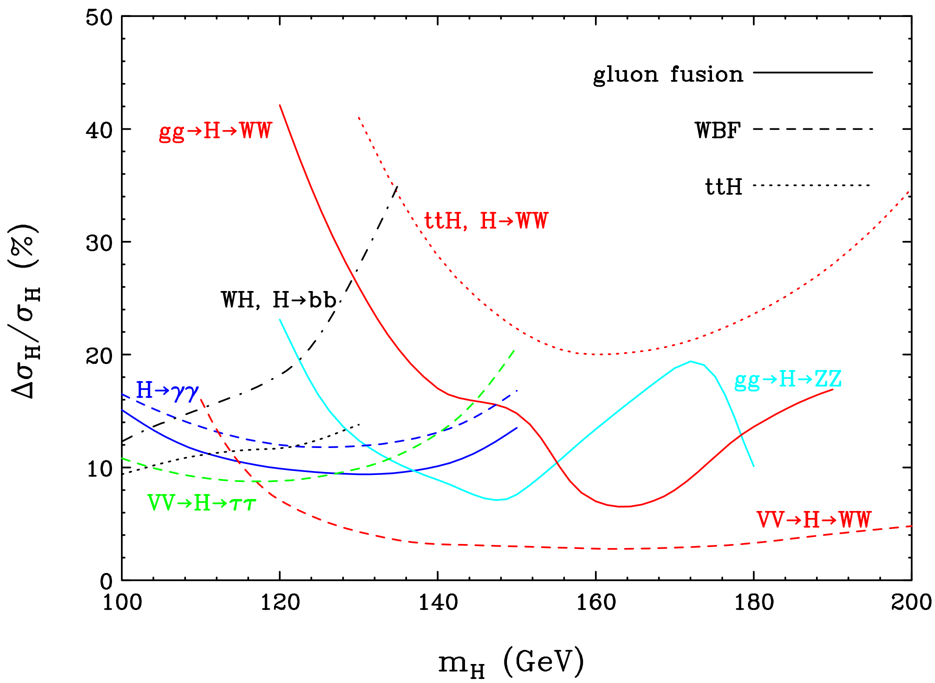

FIG. 1: Expected relative error on the determination of $B\sigma$ for various Higgs search channels at the LHC with 200 fb^{-1} of data. Solid lines are for inclusive Higgs production channels which are dominated by gluon fusion. Expectations for weak boson fusion are given by the dashed lines. The black-dotted line is for $ttH, H \to b\bar{b}$ as analyzed in Ref. [13]. The $ttH, H \to W^+W^-$ [15] (red dotted) and $WH, H \to b\bar{b}$ [16] (dash-dotted) curves assume 300 fb^{-1} of data and high luminosity running.

The particular importance of this channel is that it allows to isolate the $H \to b\bar{b}$ partial width, because the Higgs coupling to W's can be separately determined in WBF.

The statistical accuracy with which the signal cross sections of the processes in Eqs. (1-9) can be determined is shown in Fig. 1. For 100 fb^{-1} of data per experiment we expect typical statistical errors of order 10%. Experimental systematic errors, e.g. luminosity errors or knowledge of detector acceptance will be substantially smaller, of order 5% or less. This means that higher luminosity running can improve experimental errors substantially, provided that problems associated with pile-up can be overcome. Such dedicated analyses have not been finalized yet for all processes. In a conservative approach, the results below are based on a nominal integrated luminosity of 200 fb^{-1}, unless stated otherwise.

III. MEASUREMENT OF HIGGS PROPERTIES

In order to translate the cross section measurements of the various Higgs production and decay channels into measurements of Higgs boson properties, in particular into measurements of the various Higgs boson couplings to gauge fields and fermions, it is convenient to rewrite them in terms of partial widths of various Higgs boson decay channels. The Higgs-fermion couplings g_{Hff}, for example, which in the SM are given by the fermion masses, $g_{Hff} = m_f(m_H)/v$, can be traded for $\Gamma_f = \Gamma(H \to \bar{f}f)$, where, for top-quarks, the final fermions f would be virtual. Similarly, the square of the HWW coupling ($g_{HWW} = gm_W$ in the SM) or the HZZ coupling is proportional to the partial widths $\Gamma_W = \Gamma(H \to WW^*)$ or $\Gamma_Z = \Gamma(H \to ZZ^*)$. $\Gamma_\gamma = \Gamma(H \to \gamma\gamma)$ and $\Gamma_g = \Gamma(H \to gg)$ determine the squares of the effective $H\gamma\gamma$ and Hgg couplings. The Higgs production cross sections are governed by the same squares of couplings, hence, $\sigma(VV \to H) \sim \Gamma_V$ (for $V = g,\ W,\ Z$). Combined with the branching fractions $B(H \to ii) = \Gamma_i/\Gamma$ the various signal cross sections measure different combinations of Higgs boson partial and total widths, $\Gamma_i\Gamma_j/\Gamma$.

The production rate for WBF is a mixture of $ZZ \to H$ and $WW \to H$ processes, and we cannot distinguish between the two experimentally, at the LHC. In a large class of models the ratio of HWW and HZZ couplings is identical to the one in the SM, however, and this includes the MSSM. Let us therefore assume that 1) the $H \to ZZ^*$ and $H \to WW^*$ partial widths are related by SU(2) as in the SM, i.e. their ratio, z, is given by the SM value, $z = \Gamma_Z/\Gamma_W = z_{SM}$. This assumption can be tested, at the 15-20% level for $m_H > 130$ GeV, e.g. by

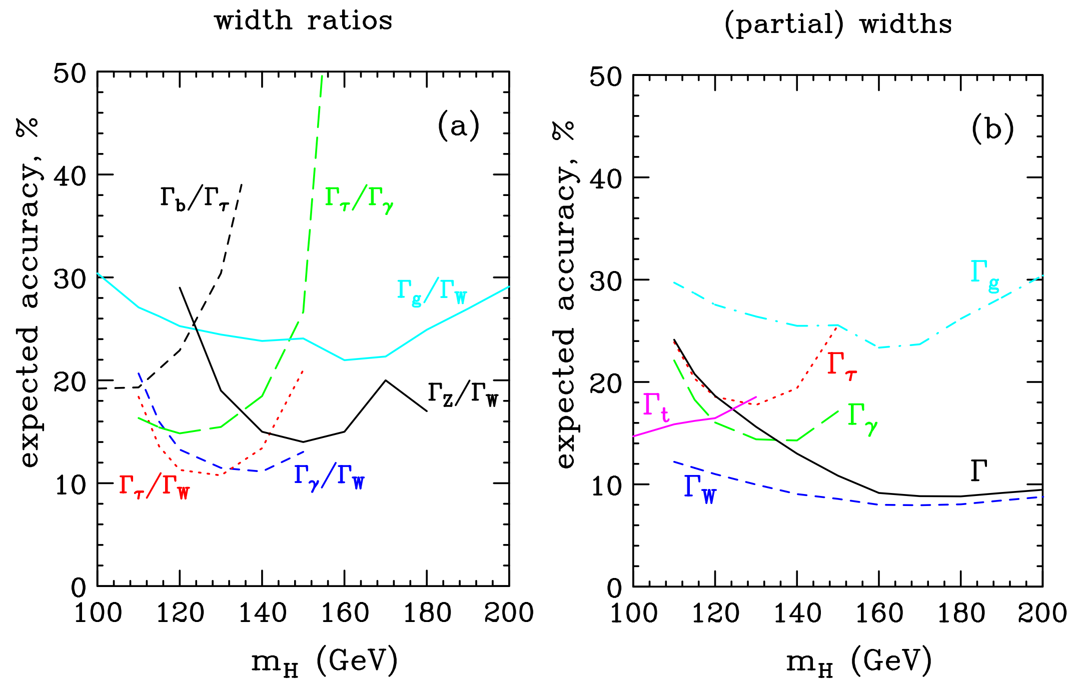

FIG. 2: Relative accuracy expected at the LHC with 200 fb^{-1} of data for (a) various ratios of Higgs boson partial widths and (b) the indirect determination of partial and total widths $\tilde{\Gamma}$ and $\tilde{\Gamma}_i = \Gamma_i(1-\epsilon)$. Width ratio extractions only assume W, Z universality, which can be tested at the 15 to 30% level (solid line). Indirect width measurements assume b, τ universality in addition and require a small branching ratio ϵ for unobserved modes like $H \to c\bar{c}$. (See text).

forming the ratio $B\sigma(gg \to H \to ZZ^*)/B\sigma(gg \to H \to WW^*)$ [5]. The expected precision, as a function of m_H, is given by the solid black line in Fig. 2.

With W, Z-universality, the three weak boson fusion cross sections give us direct measurements of three combinations of (partial) widths,

$$X_\gamma = \frac{\Gamma_W \Gamma_\gamma}{\Gamma} \qquad \text{from} \quad qq \to qqH,\ H \to \gamma\gamma\ , \tag{10}$$

$$X_\tau = \frac{\Gamma_W \Gamma_\tau}{\Gamma} \qquad \text{from} \quad qq \to qqH,\ H \to \tau\tau\ , \tag{11}$$

$$X_W = \frac{\Gamma_W^2}{\Gamma} \qquad \text{from} \quad qq \to qqH,\ H \to WW^*\ , \tag{12}$$

In addition the three gluon fusion channels provide measurements of

$$Y_\gamma = \frac{\Gamma_g \Gamma_\gamma}{\Gamma} \qquad \text{from} \quad gg \to H \to \gamma\gamma\ , \tag{13}$$

$$Y_Z = \frac{\Gamma_g \Gamma_Z}{\Gamma} \qquad \text{from} \quad gg \to H \to ZZ^*\ , \tag{14}$$

$$Y_W = \frac{\Gamma_g \Gamma_W}{\Gamma} \qquad \text{from} \quad gg \to H \to WW^*\ . \tag{15}$$

Finally, the $t\bar{t}H$ and WH associated production channels measure the combinations

$$T_b = \frac{\Gamma_t \Gamma_b}{\Gamma} \qquad \text{from} \quad gg \to t\bar{t}H,\ H \to b\bar{b}\ , \tag{16}$$

$$T_W = \frac{\Gamma_t \Gamma_W}{\Gamma} \qquad \text{from} \quad gg \to t\bar{t}H,\ H \to WW^*\ , \tag{17}$$

$$U_b = \frac{\Gamma_W \Gamma_b}{\Gamma} \qquad \text{from} \quad q\bar{q} \to WH,\ H \to b\bar{b}\ . \tag{18}$$

When extracting Higgs couplings, the QCD uncertainties of production cross sections enter. These can be estimated via the residual scale dependence of the NLO predictions and are small (below 5%) for the WBF case [17], while larger uncertainties are found for gluon fusion [18, 19]. Recently, the NNLO QCD corrections for the gluon fusion cross section have been determined [20], in the heavy top-quark limit, which provides an excellent approximation for the intermediate mass Higgs boson considered here. First results indicate a stabilization of the perturbative expansion at two loops. The diminished scale dependence at NNLO suggests a remaining error due to higher order effects of as little as 15%. The present analysis assumes a theoretical uncertainty of 20% in the gluon fusion cross section. For the $t\bar{t}H$ cross section, which has been calculated at NLO as well [21, 22], the scale dependence is reduced dramatically at NLO, to a level of about 6% [21]. For this analysis I conservatively take a theory error of 10% into account.

A first test of the Higgs sector is provided by taking ratios of the X_i's and ratios of the Y_i's. QCD uncertainties, and all other uncertainties related to the initial state, like luminosity and pdf errors, largely cancel in these ratios. For example, $X_\tau/X_W = \Gamma_\tau/\Gamma_W$ compares the $\tau\tau H$ Yukawa coupling with the HWW coupling, while X_γ/X_W and Y_γ/Y_W determine the analogous ratio, Γ_γ/Γ_W for the loop-induced photon–Higgs coupling. Expected errors on theses ratios, for 200 fb^{-1} of data, are shown in Fig. 2(a). For Higgs masses between 120 and 140 GeV they are in the 10–15% range. Accepting an additional systematic error of about 20%, a measurement of the ratio Γ_g/Γ_W, which determines the Htt to HWW coupling ratio, can be performed, by measuring the cross section ratios $B\sigma(gg \to H \to \gamma\gamma)/\sigma(qq \to qqH)B(H \to \gamma\gamma)$ and $B\sigma(gg \to H \to WW^*)/\sigma(qq \to qqH)B(H \to WW^*)$. Comparing WH to WBF cross sections, the ratio $U_b/X_\tau = \Gamma_b/\Gamma_\tau$ determines the ratio of b-quark to tau Yukawa couplings. Because QCD radiative corrections to both WBF and Drell-Yan processes are well known, this cross section ratio has a small QCD error, which is taken as 10%. Taking the error estimates of Ref. [16], for 300 fb^{-1} in one detector, and $m_H = 120$ GeV, the Γ_b/Γ_τ ratio can be determined with an overall uncertainty of $\pm 23\%$. Since this measurement becomes worse quickly with increasing m_H, it will be replaced below by the assumption of b, τ universality.

Beyond the measurement of coupling ratios, minimal additional assumptions allow an indirect measurement of the total Higgs width. First of all, the τ rate in WBF is measurable with an accuracy of order 10%. The τ is a third generation fermion with isospin $-\frac{1}{2}$, just like the b-quark. In many models, the ratio of their coupling to the Higgs is given by the τ to b mass ratio. In addition to W, Z-universality we thus assume that (2) $y = \Gamma_b/\Gamma_\tau = y_{SM}$ and, finally, (3) the branching ratio for unexpected channels is small, i.e. $\epsilon = 1 - \left[B(H \to b\bar{b}) + B(H \to \tau\tau) + B(H \to WW^*) + B(H \to ZZ^*) + B(H \to gg) + B(H \to \gamma\gamma)\right] \ll 1$. An error of 7% is assigned to the b, τ universality assumption, corresponding to the uncertainty induced in y_{SM} by the error on the b-quark mass.

With these three assumptions consider the observable

$$\begin{aligned}\tilde{\Gamma}_W &= X_\tau(1+y) + X_W(1+z) + X_\gamma + Y_W \\ &= \Big(\Gamma_\tau + \Gamma_b + \Gamma_W + \Gamma_Z + \Gamma_\gamma + \Gamma_g\Big)\frac{\Gamma_W}{\Gamma} = (1-\epsilon)\Gamma_W \;. \end{aligned} \tag{19}$$

$\tilde{\Gamma}_W$ provides a lower bound on $\Gamma(H \to WW^*) = \Gamma_W$. Provided ϵ is small (within the SM and for $m_H \geq 115$ GeV, $\epsilon < 0.03$ and it is dominated by $B(H \to c\bar{c})$), the determination of $\tilde{\Gamma}_W$ provides a direct measurement of the $H \to WW^*$ partial width. Once Γ_W has been determined, the total width of the Higgs boson is given by

$$\Gamma = \frac{\Gamma_W^2}{X_W} = \frac{1}{X_W}\Big(X_\tau(1+y) + X_W(1+z) + X_\gamma + \tilde{X}_g\Big)^2 \frac{1}{(1-\epsilon)^2} \;. \tag{20}$$

Similarly, other partial widths can be extracted by combining the ratio measurements discussed above with the Γ_W determination, e.g.

$$\tilde{\Gamma}_\tau = \frac{\Gamma_\tau}{\Gamma_W}\tilde{\Gamma}_W = \frac{X_\tau}{X_W}\tilde{\Gamma}_W \;. \tag{21}$$

The top quark Yukawa coupling can be determined by the combination

$$\tilde{\Gamma}_t = \frac{T_b}{X_\tau}\tilde{\Gamma}_W \frac{1}{y_{SM}} = \frac{\Gamma_t\Gamma_b}{\Gamma_W\Gamma_\tau}\tilde{\Gamma}_W \frac{\Gamma_\tau^{SM}}{\Gamma_b^{SM}} \;. \tag{22}$$

Extractions of Γ_τ and the total width require a measurement of the $qq \to qqH, H \to WW^*$ cross section, which is expected to be available for $m_H \gtrsim 110$ GeV [11], but suffers from poor statistics close to the limit set by LEP2. Consequently, errors are sizable for Higgs masses around 110 GeV, but stay within the 10–20% range for the most interesting Higgs mass region, between 120 and 140 GeV. Results for these indirect extractions of (partial) widths are shown in Fig. 2(b) and look highly promising.

One should note that only a few of these measurements, most notably the $H \to gg$ partial width (over the entire Higgs mass range) and the extraction of $\tilde{\Gamma}_W$ and $\tilde{\Gamma}$ for $m_H \gtrsim 150$ GeV, are limited by systematic uncertainties, in particular higher order QCD effects. For the WBF cross sections the assessment of these errors (5%) is probably too conservative. This means that substantial improvements are possible, in principle, with higher luminosity data, in the 115 GeV $< m_H <$ 150 GeV mass range. Whether pile-up effects do permit such improvements requires detailed studies.

IV. SUMMARY

With an integrated luminosity of 100 fb^{-1} per experiment, the LHC can measure various ratios of Higgs partial widths, with accuracies of order 10 to 25%. This translates into 5 to 10% measurements of various ratios of coupling constants. The ratio Γ_τ/Γ_W measures the coupling of down-type fermions relative to the Higgs couplings to gauge bosons. To the extent that the $H\gamma\gamma$ triangle diagrams are dominated by the W loop, the width ratio $\Gamma_\tau/\Gamma_\gamma$ probes the same relationship. The fermion triangles leading to an effective Hgg coupling are expected to be dominated by the top-quark, thus, Γ_g/Γ_W probes the coupling of up-type fermions relative to the HWW coupling. This top-quark Yukawa coupling can be probed directly, at the 15 to 20% level for $m_H \lesssim 130$ GeV, via $t\bar{t}H$ production with $H \to b\bar{b}$. Finally, for any Higgs boson mass in the range left by LEP2, the absolute normalization of the HWW coupling is accessible via the extraction of the $H \to WW^*$ partial width in weak boson fusion.

These measurements test the crucial aspects of the Higgs sector. The HWW coupling, being linear in the Higgs field, identifies the observed Higgs boson as the scalar responsible for the spontaneous breaking of $SU(2) \times U(1)$: a scalar without a vacuum expectation value does not exhibit such a trilinear coupling at tree level. The particular tensor structure of this SM HWW coupling can be identified as well in WBF [23]. The measurement of the ratios g_{Htt}/g_{HWW} and $g_{H\tau\tau}/g_{HWW}$ then probes the mass generation of both up and down type fermions.

These measurements may be complemented by observation of $WH/ZH,\ H \to b\bar{b}$ production at the Tevatron or the LHC to remove assumptions on the $g_{Hbb}/g_{H\tau\tau}$ coupling ratios. In all, hadron collider data in the LHC era are expected to determine the dominant couplings of a SM like Higgs boson at the 5–10% level.

Acknowledgments

This work was supported in part by WARF and in part by DOE under Grant No. DE-FG02-95ER40896.

[1] ATLAS, *Detector and physics performance Technical Design Report* (1999), CERN-LHCC-99-15, `http://atlasinfo.cern.ch/Atlas/GROUPS/PHYSICS/TDR/access.html`.
[2] G. Bayatian *et al.*, *CMS Technical Proposal* (1994), CERN-LHCC-94-38.
[3] D. Denegri *et al.*, *Summary of the CMS discovery potential for the MSSM SUSY Higgses* (2001), hep-ph/0112045.
[4] D. Charlton, *Experimental tests of the standard model* (2001), hep-ex/0110086.
[5] D. Zeppenfeld, R. Kinnunen, A. Nikitenko, and E. Richter-Was, Phys. Rev. **D62**, 013009 (2000), hep-ph/0002036.
[6] D. Rainwater and D. Zeppenfeld, JHEP **12**, 005 (1997), hep-ph/9712271.
[7] D. L. Rainwater, *Intermediate-mass Higgs searches in weak boson fusion* (1999), hep-ph/9908378.
[8] D. Rainwater, D. Zeppenfeld, and K. Hagiwara, Phys. Rev. **D59**, 014037 (1999), hep-ph/9808468.
[9] T. Plehn, D. Rainwater, and D. Zeppenfeld, Phys. Rev. **D61**, 093005 (2000), hep-ph/9911385.
[10] D. Rainwater and D. Zeppenfeld, Phys. Rev. **D60**, 113004 (1999), hep-ph/9906218.
[11] N. Kauer, T. Plehn, D. Rainwater, and D. Zeppenfeld, Phys. Lett. **B503**, 113 (2001), hep-ph/0012351.
[12] D. Cavalli *et al.*, *The Higgs working group: Summary report* (2002), hep-ph/0203056.
[13] V. Drollinger, Müller, T., and D. Denegri, *Searching for Higgs bosons in association with top quark pairs in the $H^0 \to b\bar{b}$ decay mode* (2001), hep-ph/0111312.
[14] D. Green, K. Maeshima, R. Vidal, W. Wu, and S. Kunori, *A Study of $t\bar{t}H$ at CMS*, fERMILAB-FN-0705.
[15] F. Maltoni, D. Rainwater, and S. Willenbrock, *Measuring the top-quark Yukawa coupling at hadron colliders via $t\bar{t}H, H \to W^+W^-$* (2002), hep-ph/0202205.
[16] V. Drollinger, Müller, T., and D. Denegri, *Prospects for Higgs boson searches in the channel $W^\pm H^0 \to \ell^\pm \nu b\bar{b}$* (2002), hep-ph/0201249.
[17] T. Han, G. Valencia, and S. Willenbrock, Phys. Rev. Lett. **69**, 3274 (1992), hep-ph/9206246.
[18] A. Djouadi, M. Spira, and P. M. Zerwas, Phys. Lett. **B264**, 440 (1991).
[19] M. Spira, A. Djouadi, D. Graudenz, and P. M. Zerwas, Nucl. Phys. **B453**, 17 (1995), hep-ph/9504378.
[20] R. V. Harlander and W. B. Kilgore, *NLO Higgs production at hadron colliders* (2002), hep-ph/0201206.
[21] W. Beenakker *et al.*, Phys. Rev. Lett. **87**, 201805 (2001), hep-ph/0107081.
[22] L. Reina and S. Dawson, Phys. Rev. **D65**, 053017 (2002), hep-ph/0109066.
[23] T. Plehn, D. Rainwater, and D. Zeppenfeld, Phys. Rev. Lett. **88**, 051801 (2002), hep-ph/0105325.